Analytica Chimica Acta xxx (2016) 1–8

Contents lists available at ScienceDirect

Analytica Chimica Acta

journal homepage: www.elsevier.com/locate/aca

Enzyme spheres as novel tracing tags coupled with target-induced DNAzyme assembly for ultrasensitive electrochemical microRNA assay

Yongmei Wu, Kai Sheng, Yongqin Liu, Qian Yu, Baoxian Ye*

College of Chemistry and Molecular Engineering, Zhengzhou University, Zhengzhou, 450001, PR China

HIGHLIGHTS

- A highly loaded HRP sphere was synthesized for the first time and was used as bifunctional label.
- Pd@HRP served as signal indicator and electrocatalyst for the fabrication of biosensor.
- DNAzyme-aided target recycling amplification and rolling circle amplification further amplify the signal.
- The biosensor displayed an improved sensitivity for microRNA detection.

GRAPHICAL ABSTRACT

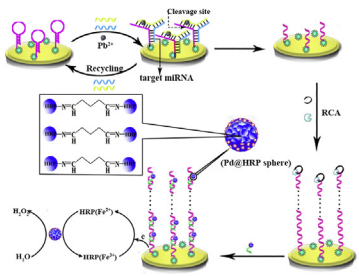

ARTICLE INFO

Article history:
Received 17 August 2016
Received in revised form
29 September 2016
Accepted 5 October 2016
Available online xxx

Keywords:
DNAzyme-aided target recycling
Horseradish peroxidase sphere
Rolling circle amplification
Electrochemical biosensor
MicroRNA

ABSTRACT

In this work, an ultrasensitive electrochemical microRNA detection strategy was developed based on porous palladium-modified horseradish peroxidase sphere (Pd@HRP) and target-induced assembly of DNAzyme. A highly loaded HRP sphere was prepared by covalent layer-by-layer assembly with $CaCO_3$ as sacrificial template for the first time, and was further modified with porous Pd. Notably, Pd@HRP composite showed a good redox activity of HRP and electrocatalytic activity toward H_2O_2. The utilization of Pd@HRP as electrochemical signal indicator and enhancer to fabricate biosensor could avoid the need for additional redox mediator and amplify the detection sensitivity. Moreover, target recycling amplification was achieved by Pb^{2+}-induced cleavage of ternary "Y" structure, circumventing the use of labile nuclease. Subsequent DNA concatamer synthesized through rolling circle amplification (RCA) reaction with cleaved hairpin probe as primer, hybridized with plentiful Pd@HRP-DNA probes, which led to the increased loading of redox-active and electrocatalytic Pd@HRP for sensitivity improvement. So the proposed electrochemical biosensor detected miRNA-24 down to 0.2 fM (S/N = 3) with a wide linear range from 3 fM to 1 nM. With bifunctional Pd@HRP tag, DNAzyme-aided target recycle and programmable junction probe, this strategy possessed the advantages of high efficiency, high sensitivity, low cost and versatility, and thus held great promise for other low-abundance nucleic acids determination.

1. Introduction

Quantification of microRNA (miRNA) regulating gene expression in various biological processes is of great significance for clinical diagnostics and prognosis [1,2]. Up until now, various assays including electrochemistry [3], fluorescence [4], chemiluminescence [5] and colorimetry [6] have been explored for sensitive detection of miRNA. Electrochemical strategies coupled with signal amplification method is often an attractive approach for the amplified biological detection because of its high sensitivity,

* Corresponding author.
E-mail address: yebx@zzu.edu.cn (B. Ye).

http://dx.doi.org/10.1016/j.aca.2016.10.005
0003-2670/

simplicity, fast response, low cost and portable electrochemical devices [7,8]. Driven by more sensitive and cost-effective diagnostics, signal amplification improvement was imperative for electrochemical biosensor to efficiently detect ever smaller quantities of biomarker.

Rolling circle amplification (RCA) is generally considered as highly sensitive and specific resulting from the RCA-synthesized DNA concatamers capable of binding more signal probes [9–12]. Unfortunately, involvement of multiple monofunctional tags in reported signal probe presents a risk for sample contamination and causes the complexity and limited efficiency of bioassay. Redox enzyme such as horseradish peroxidase (HRP) is the most promising candidate for resolving the above issues, considering its intrinsic redox center and biocatalytic activity. Compared with a free enzyme, highly loaded enzyme structure is preferable to the construction of high-efficiency biosensor owing to the positive effect of the quantity of enzyme on its amplification efficiency and direct electrochemistry [13]. Recently, the biocompatible calcium carbonate ($CaCO_3$) with high loading capacity has been exploited as ideal template to increase redox enzyme loading in biosensor [14–16]. Furthermore, based on their biocompatibility, conductivity and affinity to amino-containing biomolecules, noble metal nanomaterials can provide a microenvironment to keep biomolecular bioactivity and can be used to modify protein for their direct electrochemistry [17–19]. Therefore, it is conceivable that porous palladium (Pd) is conducive to realize the direct electron transfer of enzyme and its catalytic property makes it extremely absorbing as electrocatalyst for signal amplification [18]. And porous structure makes nanomaterial render larger surface area for efficient immobilization of biomolecules and much higher catalytic performance for substrate in contrast to its solid counterparts [20,21]. In this work, a highly loaded HRP sphere was synthesized by covalent layer-by-layer (LbL) assembly with $CaCO_3$ as a sacrificial template for the first time, and was further functionalized with porous Pd. The composite may reveal electroactivity and electrocatalysis, which contributes to its potential use in electrochemical biosensor. The integration of Pd@HRP-tagged signal probe with RCA holds promise for enhancing the efficiency of biosensor and amplifying the biological detection.

Another effective approach to amplify signal is to use target recycling. Despite these attainments in target recycling-oriented amplification [22–24], most of them involve the use of expensive and labile nicking endonuclease or exonuclease, which may lead to a high cost and a false signal due to the inactivation of nucleases. In contrast, Pb^{2+}-specific DNAzyme exhibits some advantages over nucleases such as high catalytic activity, good stability and inexpensive components [25], but its sequence-specific components restrict the application in electrochemical biosensor. Y junction-based detection platforms relying on three complementary oligonucleotide branches can circumvent the sequence-specific limitation and guarantee flexibility toward various analytes [26–28]. In these methods, specific strand can be recycled through assistance of nucleases, causing the detection of amplification, but these approaches still suffered the drawback of increased cost and susceptibility of nuclease. In this work, Y junction probe was designed for the assembly of Pb^{2+}-specific DNAzyme, aiming at achieving DNAzyme-aided target recycling without nuclease requirement.

Inspired by these, an electrochemical bioassay was reported here for sensitive detection of miRNA-24 (as a model analyte) by using Pd@HRP tag and DNAzyme-aided target recycling amplification (Scheme 1). When target miRNA was present, the HP, target and auxiliary probe (AP) hybridized to form a ternary Y junction structure on the sensor interface. Notably, HP/AP hybrid branch acted as the assembled DNAzyme to cleave the ribonucleotide-containing HP with the aid of Pb^{2+}, resulting in the DNAzyme-aided target recycling signal amplification. At the same time, the remaining hairpin probe functioned as primer to synthesize DNA concatamer via RCA reaction. Then, RCA-amplified concatamer served as a powerful scaffold for increasing the signal probe (Pd@HRP-DNA probe) loading, which was beneficial to the enhancement of electrochemical signal. It should be noted that the signal was obtained from HRP without requiring additional redox mediators. Furthermore, the electrocatalysis of Pd@HRP composites toward H_2O_2 reduction could further improve the signal intensity and sensitivity of biosensor.

2. Experimental

2.1. Materials and reagents

Potassium tetrachloropalladate(II) (K_2PdCl_4, 99%), Gold chloride ($HAuCl_4$), horseradish peroxidase (HRP) and 6-mercaptohexanol (MCH) were purchased from Sigma-Aldrich. Chemical Co. (St. Louis, MO, USA). Cetyltrimethylammonium chloride (CTAC), ascorbic acid (AA) and polyethylenimine (PEI) were obtained from J&K Scientific Ltd. (Beijing, China). Glutaraldehyde (GA), ethylenediamine tetraacetic acid disodium salt (Na_2EDTA), $NaBH_4$, tris-hydroxymethylaminomethane hydrochloride (Tris-HCl) and tris(2-carboxyethyl) phosphine hydrochloride (TCEP) were obtained from Aladdin Co. Ltd. (Shanghai, China). T4 DNA Ligase, T4 DNA Ligase buffer, dNTP mixture, phi 29 DNA polymerase and RCA reaction buffer were supplied by Thermo Fisher Scientific Inc (Shanghai, China). The ultrapure water with specific resistance of 18.2 MΩ cm was used throughout the experiment. Working buffer: phosphate buffered solution (PBS, pH 7.0, 0.1 M) was prepared with 0.1 M Na_2HPO_4, 0.1 M KH_2PO_4, and 2.0 mM $MgCl_2$. Immobilization buffer (IB): 10 mM Tris-HCl, 1 mM EDTA, 10 mM TCEP, 0.1 M NaCl, (pH 7.4). Hybridization buffer (HB): 10 mM Tris-HCl, 1.0 mM EDTA, 1.0 M NaCl (pH 7.0). HPLC-purified microRNAs were synthesized by Takara Biotechnology Co., Ltd. (Dalian, China) and other DNA probes were obtained from Sangon, Biotech Co., Ltd. (Shanghai, China). 1 × TE buffer (10 mM Tris-HCl, 1.0 mM EDTA, pH 8.0) was used to dissolve and store all oligonucleotides. The nucleotide sequences were listed in Table S1 (see Supplementary material).

2.2. Apparatus

Scanning electron microscopy (SEM, JEOL, JSM-7500F) with energy-dispersive spectrometer (EDS) and transmission electron microscope (TEM, USA FEI, M3000) were performed to characterize the materials. The pH measurement was carried out with a PHS-3C precision pH meter (Shanghai, China). All the electrochemical measurements were performed with a CHI 650A electrochemical workstation (Shanghai Chenhua Instrument, China). A conventional three-electrode system was used, including the modified glassy carbon electrode (GCE, $\Phi = 4$ mm) as working electrode, platinum wire as counter electrode and Ag/AgCl electrode as reference electrode respectively.

2.3. Synthesis of Pd@HRP composite

For the synthesis of Pd@HRP labels, porous Pd was first prepared based on a seed-mediated method [29]. The high-content HRP sphere was prepared by the decomposable porous $CaCO_3$-templated assembly technique described in Ref. [30] with slight modification. Based on the high affinity between Pd and amino group from enzyme, porous Pd could be decorated onto the HRP spheres. The schematic diagram in Scheme 1 illustrated the preparation of Pd@HRP composite. The detail procedures for the synthesis of all materials were described in Supporting Information.

Please cite this article in press as: Y. Wu, et al., Enzyme spheres as novel tracing tags coupled with target-induced DNAzyme assembly for ultrasensitive electrochemical microRNA assay, Analytica Chimica Acta (2016), http://dx.doi.org/10.1016/j.aca.2016.10.005

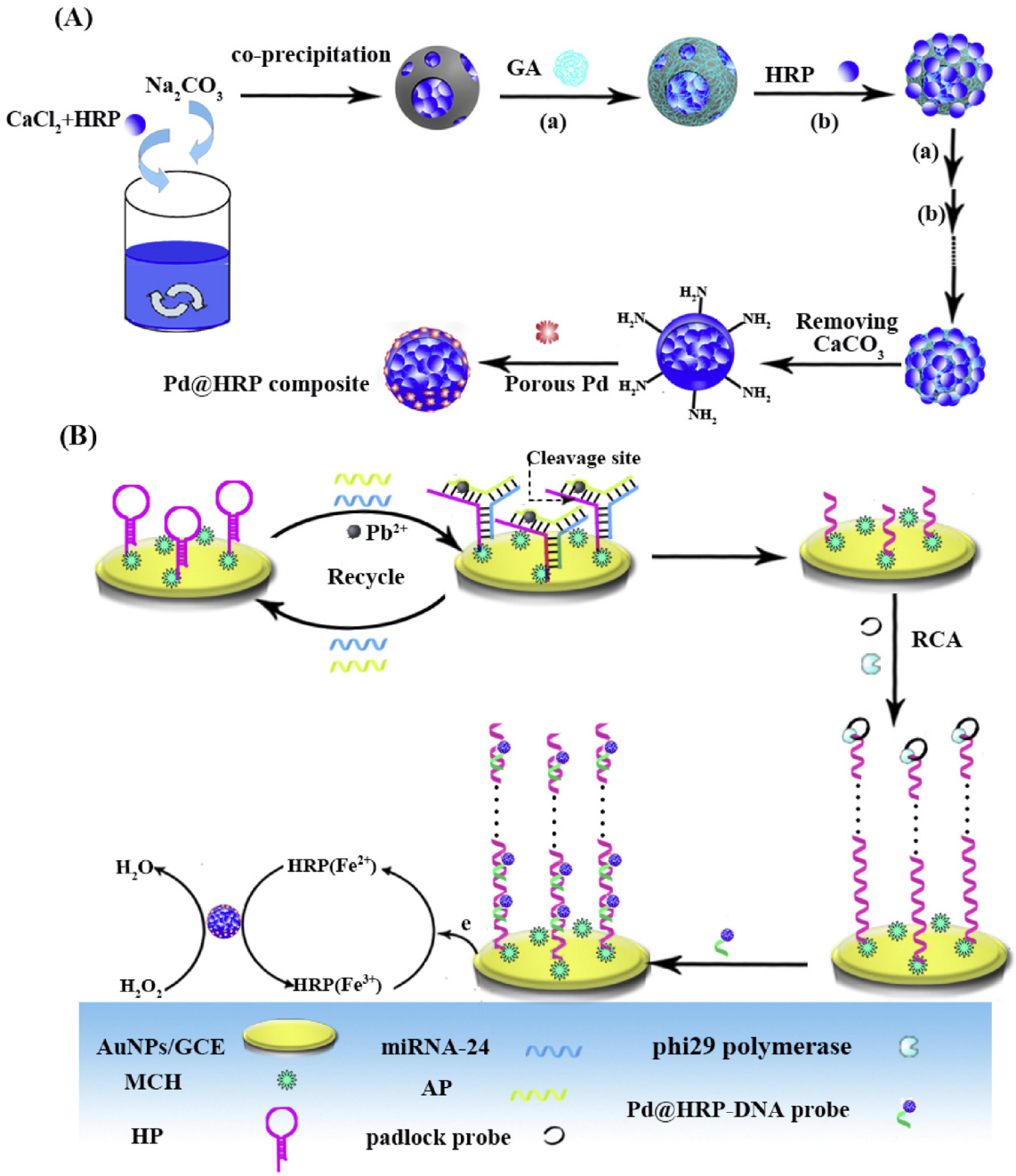

Scheme 1. (A) The synthesis of Pd@HRP composite and (B) Electrochemical miRNA sensing based on Pd@HRP as signal tag and electrocatalyst coupled with DNAzyme-aided target recycling amplification.

2.4. Preparation of Pd@HRP-tagged oligonucleotide probe (Pd@HRP-DNA probe)

The amino-tethered oligonucleotide probe (100 μL, 2.5 μM) was mixed with 2 mL of Pd@HRP composite in PBS (pH 7.0), and then the mixture was gently stirred overnight at 4 °C. The oligonucleotide probe could be conjugated to Pd@HRP composites since Pd nanoparticle has high affinity for amino group of probe. Pd@HRP-DNA probe was collected by centrifugation and resuspended in PBS prior to use. For the synthesis of porous Pd-tagged oligonucleotide probe (Pd-DNA probe), a similar procedure was employed, except for the substitution of Pd@HRP composite by porous Pd.

2.5. Construction of electrochemical biosensor

Prior to modification, the bare GCE was polished to mirror-like with 0.3 and 0.05 μm Al_2O_3 powder and sonicated with ethanol and water, respectively. The pretreated GCE was then modified with AuNPs by electrodeposition in $HAuCl_4$ (1 wt %) at −0.2 V for 30 s. The assembled AuNPs have the flower-shaped morphology with average size of about 500 nm (Fig. S1). Before probe immobilization, thiolated hairpin probe (HP) was heated to 95 °C for 2 min first. After cooled to room temperature, the thiolated probe (1 μM, 10 μL) was dripped onto the AuNPs/GCE and incubated overnight at room temperature in 100% humidity. After that, the

Please cite this article in press as: Y. Wu, et al., Enzyme spheres as novel tracing tags coupled with target-induced DNAzyme assembly for ultrasensitive electrochemical microRNA assay, Analytica Chimica Acta (2016), http://dx.doi.org/10.1016/j.aca.2016.10.005

resulting electrode was treated with MCH (1 mM) to block the unoccupied site of electrode surface. Also, MCH acted as spacer thiol to help oligonucleotide probe "stand" up at the electrode surface, a configuration favorable to subsequent nucleic acid hybridization [31]. Thorough rinsing with ultrapure water was executed after every modification.

2.6. Target-induced DNAzyme assembly and Pd@HRP tag for amplified electrochemical miRNA assay

The MCH/HP/AuNPs/GCE electrode was immersed into 10 μL of HB containing miRNA-24 with different concentration and 1 μM AP. After incubation of 16 h at room temperature, Y junction structure was formed on the electrode surface by the hybridization of HP with target and AP. Pb^{2+} (10 μL, 2 μM) was then pipetted onto the electrode and incubated at 37 °C for 1 h, followed by washing with ultrapure water. After that, a total volume 10 μL of solution containing 1 × ligase buffer (40 mM Tris-HCl, 10 mM $MgCl_2$, 10 mM DTT and 0.5 mM ATP, pH 7.8), 0.2 U T4 DNA ligase and 50 nM padlock probe, was interacted with the modified electrode at 37 °C for 1 h. During the process, 5'-phosphated padlock probe was cyclized via DNA ligation to form RCA template. T4 ligase was then inactive at 65 °C for 10 min and the electrode was rinsed with ultrapure water. RCA reaction was then performed in 10 μL of 1 × reaction buffer (33 mM Tris-acetate, 10 mM Mg-acetate, 66 mM K-acetate, 0.1% Tween 20 and 1 mM DTT) with 1 mM dNTP and 0.2 U phi29 polymerase at 37 °C for 1 h. Afterwards, the electrode was incubated for 10 min at 65 °C to inactive the polymerase, followed by rinsing with ultrapure water. And then 30 μL of Pd@HRP-DNA probes hybridized with RCA product at 37 °C for 1 h. After washed with ultrapure water, the resulting electrode was placed in 2 mL PBS (0.1 M, pH 7.0) with 1.2 mM H_2O_2 for differential pulse voltammetry (DPV) measurements with the scanning potential from 0.2 to −0.7 V (vs Ag/AgCl), modulation amplitude of 0.05 V and pulse width of 0.05 s.

3. Results and discussion

3.1. Characterization of materials

To verify the successful synthesis of HRP sphere, porous Pd and Pd@HRP composite, TEM and SEM with EDX measurement, were performed. As seen in Fig. 1A, a clear porous morphology was visible on the obtained Pd nanoparticle and the average size was about 22 nm, indicating the successful preparation of porous Pd nanostructure. From Fig. 1B, we could see that the HRP-based structure materials presented an irregularly spherical morphology with roughened surface. The inset image verified that the obtained HRP spheres were uniform and monodisperse. So it could be concluded that HRP sphere was successfully synthesized by using porous $CaCO_3$ as template and LbL assembly technique. After modification with porous Pd, the surface morphology of composite was observed by SEM. And EDS analysis was performed to ascertain chemical composition of Pd@HRP composite. As shown in Fig. 1C, porous Pd nanoparticles as bright spots (black arrow) were successfully attached to the HRP spheres. EDS date in Fig. 1C demonstrated that Pd, Fe, N, C, O and N element existed in the composite, and the weight percents against them were 5.41, 1.15, 10.21, 39.59 and 43.63, respectively. The high loading concentration of HRP might be ascribed to the effective encapsulation of enzyme into porous template and additional enzyme assembly on the template shell [14,15]. All the results confirmed the successful synthesis of Pd@HRP composite.

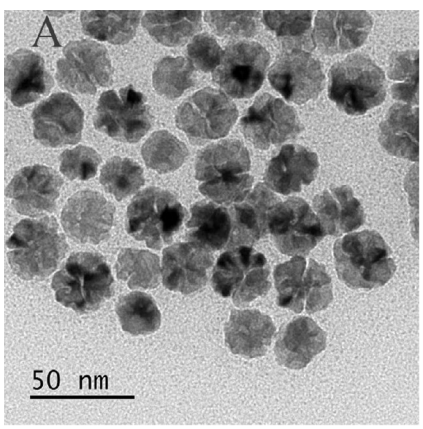

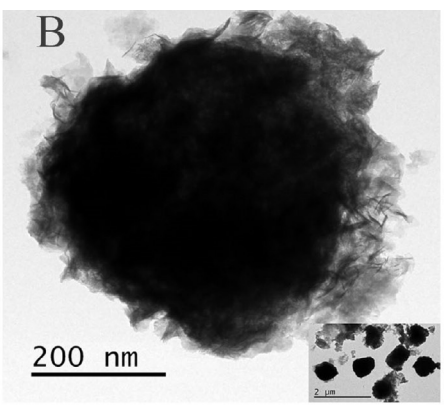

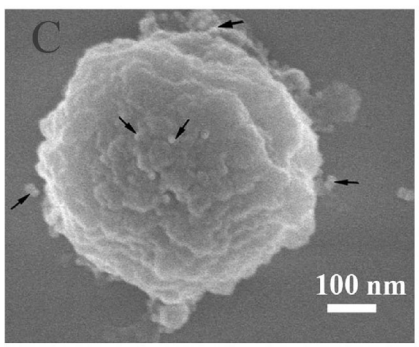

ELAN	Series	unn.C [wt. %]	norm. C [wt. %]	Atom.C [wt. %]
O 8	K-series	43.63	43.63	39.96
C 6	K-series	39.59	39.59	48.31
N 7	K-series	10.21	10.21	10.68
Fe 8	K-series	1.15	1.15	0.30
Pd 8	K-series	5.41	5.41	0.75

Fig. 1. TEM images of the porous Pd (A) and HRP spheres (B). (C): SEM image of Pd@HRP composites and its EDS analysis.

Please cite this article in press as: Y. Wu, et al., Enzyme spheres as novel tracing tags coupled with target-induced DNAzyme assembly for ultrasensitive electrochemical microRNA assay, Analytica Chimica Acta (2016), http://dx.doi.org/10.1016/j.aca.2016.10.005

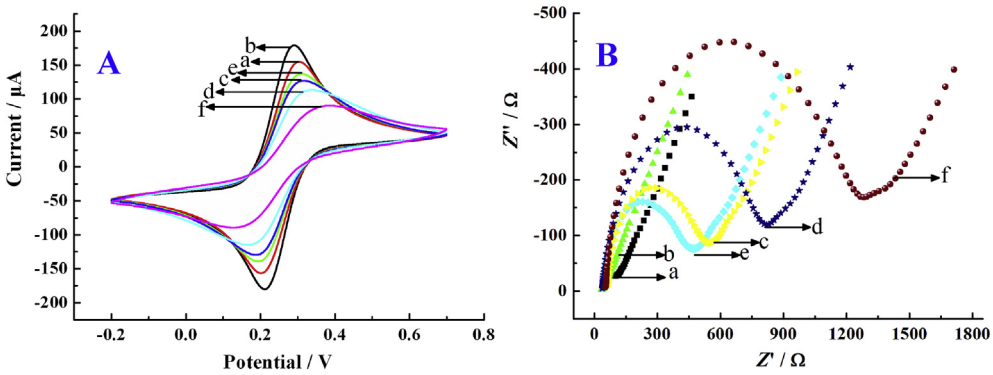

Fig. 2. (A) CV and (B) EIS characterization of (a) bare GCE, (b) AuNPs/GCE, (c) MCH/HP/AuNPs/GCE, (d) target + AP/MCH/HP/AuNPs/GCE, (e) Pb^{2+}/target + AP/MCH/HP/AuNPs/GCE, (f) RCA/Pb^{2+}/target + AP/MCH/HP/AuNPs/GCE in PBS (pH 7.0) with 5 mM $[Fe(CN)_6]^{3-/4-}$. The potential range of CV measurement was from −0.2–0.7 V (vs. Ag/AgCl) and the scan rate was 50 mV s^{-1}. EIS parameters were as follows: initial potential of 0.22 V; amplitude of 5 mV; frequency range of 0.1 Hz–100 KHz.

3.2. Electrochemical characterization of the modified electrode

The stepwise assembly process for the biosensor interface was demonstrated by cyclic voltammetry (CV) and electrochemical impedance spectroscopy (EIS) techniques. From Fig. 2A, we could see that a well-defined redox peak from $[Fe(CN)_6]^{3-/4-}$ was observed at the bare GCE (curve a). After electrodeposition of AuNPs, the current signal enhanced (curve b), indicative of fast electron transfer due to the good electroconductivity of AuNPs. The assembly of hairpin probe decreased the current signal, because the negatively charged phosphate backbone of probe was electrostatically repulsive to the $[Fe(CN)_6]^{3-/4-}$ (curve c). The signal intensity further declined after incubation with target and auxiliary probe (curve d), which might be ascribed to the increase of negatively charged nucleic acid chain or the steric hindrance effect of ternary junction on the electrode surface. The addition of Pb^{2+} resulted in an increased signal in contrast to the curve d (curve e), implying that the Pb^{2+}-induced cleavage of junction probe weakened the electrostatic repulsion to $[Fe(CN)_6]^{3-/4-}$. When RCA reaction occurred on the sensing interface, the signal sharply fell off owing to the generation of concatameric DNA product (curve f). The consistent experiment results were revealed by the EIS measurements (Fig. 2B).

3.3. Feasibility study of signal amplification

To study the availability of the amplified strategy, we performed the DPV measurement using the biosensor (i.e., MCH/HP/AuNPs/GCE) with/without miRNA (0.1 nM) in the presence/absence of Pb^{2+}, RCA and H_2O_2. As shown in Fig. 3A, neither Y junction nor RCA reaction existed in the absence of target miRNA, and thus no detectable signal was found (curve a). In the absence of Pb^{2+}, the DNAzyme kept inactivated, and thus Y junction did not dissociate as well as RCA reaction would not occur. In that case, Pd@HRP-tagged detection probes were not introduced into the system, resulting in the negligible signal (curve b). The same experimental results were also reflected in the case without RCA despite the presence of Pb^{2+} (curve c). But in the presence of target, Pb^{2+} and RCA, a strong electrochemical signal was observed at around −0.25 V (curve d) in comparison to curve a, b, c. The results indicated the high-efficiency signal amplification resulting from DNAzyme-aided target recycling and RCA. After addition of H_2O_2 in the working buffer (PBS), the peak current greatly enhanced (curve e) in comparison to that of curve d, revealing the excellent ability of Pd@HRP to amplify the electrochemical signal. The catalytic mechanism can be explained as following Eqs. (1)–(3) [32,33]. The electrode was considered as an electron donor.

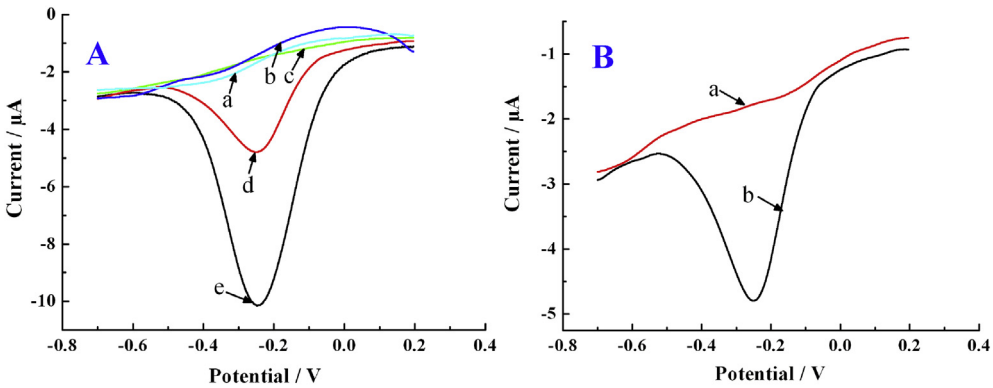

Fig. 3. (A) DPV responses of the different sensing interfaces with absence of (a) target, (b) Pb^{2+}, (c) RCA, (d) presence of 0.1 nM target and 2 μM Pb^{2+} followed by RCA in PBS (pH 7.0), (e): (d) adding 1.2 mM H_2O_2. (B) DPV responses of the biosensors in PBS (pH 7.0) toward 0.1 nM target incubated with (a) porous Pd-DNA probe and (b) Pd@HRP-DNA probe, respectively.

Please cite this article in press as: Y. Wu, et al., Enzyme spheres as novel tracing tags coupled with target-induced DNAzyme assembly for ultrasensitive electrochemical microRNA assay, Analytica Chimica Acta (2016), http://dx.doi.org/10.1016/j.aca.2016.10.005

$$\text{Pd@HRP}\left(Fe^{3+}\right) + H_2O_2 \rightarrow \text{Compound I}\left(Fe^{4+}=O,\ R^{\bullet+}\right) + H_2O \quad (1)$$

$$\text{Compound I}\left(Fe^{4+}=O,\ R^{\bullet+}\right) + e + H^+ \rightarrow \text{Compound II}\left(Fe^{4+}=O\right) \quad (2)$$

$$\text{Compound II}\left(Fe^{4+}=O\right) + e + H^+ \rightarrow \text{Pd@HRP}\left(Fe^{3+}\right) + H_2O \quad (3)$$

Additionally, Pd-DNA probe and Pd@HRP-DNA probe were used to verify the current signal originated from HRP. As shown in Fig. 3B, no electrochemical signal was observed at the electrode with porous Pd-DNA probe (curve a) because of the lack of redox mediators. By comparison, the electrode with Pd@HRP-DNA probe exhibited an obvious electrochemical signal at the potential of −0.25 V (curve b), which explained the favorable redox activity of Pd@HRP. The peak current was correspondent to the reduction process of heme group in HRP, which indicated the effective direct electron transfer between HRP and electrode and could be expressed as the following equation HRP (Fe^{3+}) + e^- → HRP (Fe^{2+}) [32,34,35]. Thus, unlike previous signal probe-coupled RCA based signal amplification approaches [7–10], this strategy hybridized a more efficient signal probe to the RCA product since Pd@HRP tag simultaneously acted as signal indicator and electrocatalyst. Using the bifunctional label to construct biosensor obviated the need for additional electroactive species and resulted in a simple bioassay with high sensitivity.

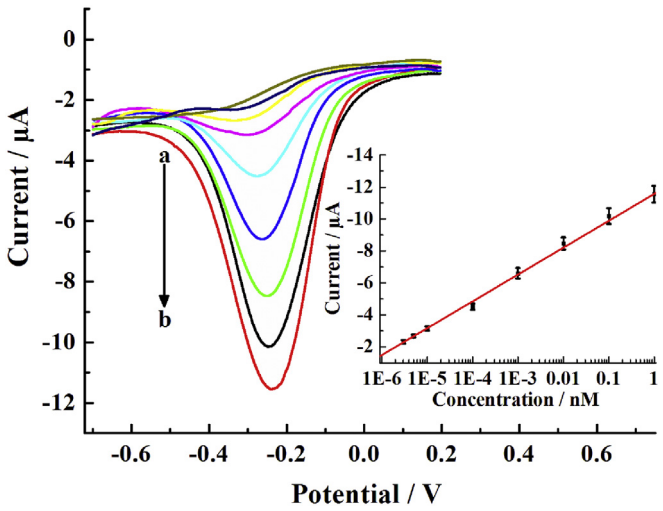

Fig. 4. DPV responses of the biosensor toward miRNA-24 with different concentration (from a to b: 0 fM, 3 fM, 5 fM, 10 fM, 100 fM, 1 pM, 10 pM, 0.1 nM and 1 nM, respectively) in PBS (0.1 M, pH 7.0) containing H_2O_2 (1.2 mM) and the resultant calibration curve for target miRNA-24.

3.4. Quantification of target miRNA-24 with the biosensor

Under the optimal experimental conditions (Fig. S2), the biosensor was applied to the quantitative analysis of miRNA-24 to assess its analytical performance. Fig. 4 showed the DPV curves of the biosensor with different concentration of target miRNA in PBS containing 1.2 mM H_2O_2. It could be seen that DPV signals gradually enhanced with the increasing miRNA concentration from 3 fM to 1 nM. The results were in accordance with the designed strategy as we expected. The higher concentration of miRNA could result in the formation of many Pb^{2+}-required DNAzymes and then production of a large quantity of primers through DNAzyme-aided cleavage reaction, ultimately leading to the synthesis of abundant RCA products and thus an enhanced current signal due to the binding of more Pd@HRP-DNA probes to RCA products. The inset in Fig. 4 indicated a good linear relationship between current intensity and the logarithm of target concentration. The corresponding regression equation was $I\,(\mu A) = -1.6815 \log c_{\text{miRNA-24}} - 11.573$ with a correlation coefficient of 0.9978. The detection limit was estimated to be 0.2 fM with 3 times the standard deviation. We also compared the performance of the proposed strategy with those of some previously reported methods [31–37] for detection of miRNA. The results in Table 1 indicated that the detection limit and the quantitative range of this strategy were comparable or even more superior.

3.5. Specificity, stability and reproducibility of the biosensor

In order to evaluate the selectivity of biosensor, other ssDNA and miRNAs, i.e., carcinoembryonic antigen binding aptamer (Apt-CEA), miRNA-29 and single base-mismatched miRNA, instead of target miRNA-24, were applied to the biosensor, respectively. As illustrated in Fig. 5, the electrochemical response for the every control group was negligible in contrast to that of target (columns a, b, c, d), although the concentration was 10-fold greater over the target. When the target was mixed with these potential interferents, the obtained signal response for the mixture was almost the same as that for target only (columns e, f). Such comparison demonstrated that the above substances had negligible influence on miRNA-24 analysis. Thus, the developed biosensor exhibited good selectivity and high specificity toward target miRNA. After the biosensor was incubated with hairpin probe, its CV response in 5 mM $[Fe(CN)6]^{3-/4-}$ solution was investigated by 50 continuous cycle scans (Fig. S3). A 5.82% decrease of initial peak current was obtained, indicating the acceptable stability of the developed biosensor. The reproducibility of the biosensor was investigated by using five equally biosensors to detect 0.1 nM target miRNA. Similar current intensity was obtained with a relative standard deviation (RSD) of 3.92%, indicating the acceptable reproducibility of the biosensor.

Table 1
Comparision of various methods for miRNA detection.

Analytical method	Detection limit	Linear range	Reference
Chronoamperometry	3 fM	10 fM – 5 pM	[36]
DPV	84.3 fM	0.1 pM – 0.5 nM	[37]
Chemiluminescene	70 pM	100 pM – 1 mM	[38]
Electrochemiluminescence	0.83 fM	2.5 fM – 50 pM	[39]
Colorimetric	27 fM	50 fM – 50 nM	[40]
Fluorescence	100 fM	1 pM – 50 pM	[41]
Surface plasmon resonance imaging	1 fM	0 pM – 50 pM	[42]
DPV	0.2 fM	3 fM–1 nM	This work

Please cite this article in press as: Y. Wu, et al., Enzyme spheres as novel tracing tags coupled with target-induced DNAzyme assembly for ultrasensitive electrochemical microRNA assay, Analytica Chimica Acta (2016), http://dx.doi.org/10.1016/j.aca.2016.10.005

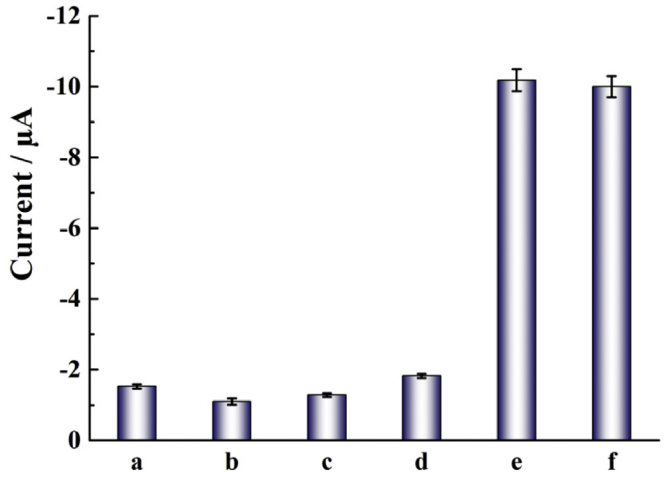

Fig. 5. Selectivity of the biosensor toward miRNA-24: (a) Blank, (b) Apt-CEA (1 nM), (c) miRNA-29(1 nM), (d) single base-mismatched miRNA(1 nM), (e) miRNA-24 (0.1 nM), (f) the mixture containing miRNA-24 and the three interferents. (Error bars represented SD, n = 3).

4. Conclusion

In summary, we synthesized novel Pd@HRP label and combined it with target-induced assembly of DNAzyme to develop ultrasensitive electrochemical biosensor. The Pd@HRP composite offered a detectable electrochemical signal and self-enhanced the signal. The use of Pd@HRP for the construction of biosensor eliminated the need for extra redox mediator and resulted in a simple bioassay with high sensitivity. Ternary junction structure was designed ingeniously for DNAzyme assembly, by which target recycling signal amplification was accomplished by DNAzyme rather than costly and liable protein-based enzyme. Meanwhile, the binding of RCA-amplified ssDNA concatamer with abundant Pd@HRP-DNA probes ensured a strong electrochemical signal output. And the electrocatalysis of Pd@HRP further amplify the response signal. As a result, the proposed bioassay exhibited a lower detection of 0.2 fM limit for miRNA analysis in range of 3 fM to 1 nM. With good stability, high specificity and sensitivity, the proposed strategy became a promising choice for the nucleic acid diagnostics in clinical.

Acknowledgements

This work was supported by the National Natural Science Foundation (NNSF) of China (21575130).

Appendix A. Supplementary data

Supplementary data related to this article can be found at http://dx.doi.org/10.1016/j.aca.2016.10.005.

References

[1] M.A. Valencia-Sanchez, J. Liu, G.J. Hannon, R. Parker, Control of translation and mRNA degradation by miRNAs and siRNAs, Genes Dev. 20 (2006) 515–524.
[2] N. Pencheva, S.F. Tavazoie, Control of metastatic progression by microRNA regulatory networks, Nat. Cell Biol. 15 (2013) 546–554.
[3] H.L. Shuai, K.J. Huang, L.L. Xing, Y.X. Chen, Ultrasensitive electrochemical sensing platform for microRNA based on tungsten oxide-graphene composites coupling with catalyzed hairpin assembly target recycling and enzyme signal amplification, Biosens. Bioelectron. 86 (2016) 337–345.
[4] R. Huang, Y.H. Liao, X.M. Zhou, D. Xing, Toehold-mediated nonenzymatic amplification circuit on grapheme oxide fluorescence switching platform for sensitive and homogeneous microRNA detection, Anal. Chim. Acta 888 (2015) 162–172.
[5] X.R. Zhang, H.X. Liu, R.J. Li, N.B. Zhang, Y. Xiong, S.Y. Niu, Chemiluminescence detection of DNA/MicroRNA based on cation-exchange of CuS nanoparticles and rolling circle amplification, Chem. Commun. 51 (2015) 6952–6955.
[6] K.J. Huang, Y.J. Liu, J.Z. Zhang, J.T. Cao, Y.M. Liu, Aptamer/Au nanoparticles/cobalt sulfide nanosheets biosensor for 17β-estradiol detection using a guanine-rich complementary DNA sequence for signal amplification, Biosens. Bioelectron. 67 (2015) 184–191.
[7] K.J. Huang, H.L. Shuai, J.Z. Zhang, Ultrasensitive sensing platform for platelet-derived growth factor BB detection based on layered molybdenum selenide–grapheme composites and Exonuclease III assisted signal amplification, Biosens. Bioelectron. 77 (2016) 69–75.
[8] W. Shen, H.M. Deng, Y.Q. Ren, Z.Q. Gao, A real-time colorimetric assay for label-free detection of microRNAs down to sub-femtomolar levels, Chem. Commun. 49 (2013) 4959–4961.
[9] Q.L. Sheng, N. Cheng, W.S. Bai, J.B. Zheng, Ultrasensitive electrochemical detection of breast cancer cell based on DNA-rolling-circle-amplification-directed enzyme-catalyzed polymerization, Chem. Commun. 51 (2015) 2114–2117.
[10] B.Q. Liu, B. Zhang, G.N. Chen, H.H. Yang, D.P. Tang, Proximity ligation assay with three-way junction-induced rolling circle amplification for ultrasensitive electronic monitoring of concanavalin A, Anal. Chem. 86 (2014) 7773–7781.
[11] H.L. Su, R. Yuan, Y.Q. Chai, L. Mao, Y. Zhuo, Ferrocenemonocarboxylic -HRP@Pt nanoparticles labeled RCA for multiple amplification of electro-immunosensing, Biosens. Bioelectron. 26 (2011) 4601–4604.
[12] Y.J. Wang, X.N. Bai, W. Wen, X.H. Zhang, S.F. Wang, Ultrasensitive electrochemical biosensor for HIV gene detection based on graphene stabilized gold nanoclusters with exonuclease amplification, ACS Appl. Mater. Interfaces 7 (2015) 18872–18879.
[13] J. Das, K. Jo, J.W. Lee, H. Yang, Electrochemical immunosensor using p-Aminophenol redox cycling by hydrazine combined with a low background current, Anal. Chem. 79 (2007) 2790–2796.
[14] X.L. Wang, Z.Y. Jiang, J.F. Shi, Y.P. Liang, C.H. Zhang, H. Wu, Metal–organic coordination-enabled layer-by-layer self-assembly to prepare hybrid microcapsules for efficient enzyme immobilization, ACS Appl. Mater. Interfaces 4 (2012) 3476–3483.
[15] Z.X. Zhao, X.S. Wang, X. Qin, Q. Chen, J.I. Anzai, Enzyme microcapsules with substrate selective permeability constructed via layer-by-layer polyelectrolyte self-assembly, Mater. Sci. Eng. C 32 (2012) 569–573.
[16] J. Peng, L.N. Feng, K. Zhang, X.H. Li, L.P. Jiang, J.J. Zhu, Calcium carbonate–gold nanocluster hybrid spheres: synthesis and versatile application in immunoassays, Chem. Eur. J. 18 (2012) 5261–5268.
[17] D. Brondani, B. Souza, B.S. Souza, A. Neves, I.C. Vieira, PEI-coated gold nanoparticles decorated with laccase: a new platform for direct electrochemistry of enzymes and biosensing applications, Biosens. Bioelectron. 42 (2013) 242–247.
[18] M. Baghayeri, H. Veisi, Fabrication of a facile electrochemical biosensor for hydrogen peroxide using efficient catalysis of hemoglobin on the porous Pd@Fe_3O_4-MWCNT nanocomposite, Biosens. Bioelectron. 74 (2015) 190–198.
[19] Y.M. Wu, W.J. Xu, L.J. Bai, Y.L. Yuan, H.Y. Yi, Y.Q. Chai, R. Yuan, Ultrasensitive thrombin detection based on direct electrochemistry of highly loaded hemoglobin spheres-encapsulated platinum nanoparticles as labels and electrocatalysts, Biosens. Bioelectron. 50 (2013) 50–56.
[20] Q. Zhou, Y.X. Lin, Y.P. Lin, Q.H. Wei, G.N. Chen, D.P. Tang, Highly sensitive electrochemical sensing platform for lead ion based on synergetic catalysis of DNAzyme and Au–Pd porous bimetallic nanostructures, Biosens. Bioelectron. 78 (2016) 236–243.
[21] S.G. Ge, E. Liu, W.Y. Liu, M. Yan, X.R. Song, J.H. Yu, Colorimetric assay of K-562 cells based on folic acid-conjugated porous bimetallic Pd@Au nanoparticles for point-of-care testing, Chem. Commun. 50 (2014) 475–477.
[22] F.L. Gao, Y. Du, J.W. Yao, Y.Z. Zhang, J. Gao, A novel electrochemical biosensor for DNA detection based on exonuclease III-assisted target recycling and rolling circle amplification, RSC Adv. 5 (2015) 9123–9129.
[23] Y. Tan, X.F. Wei, M.M. Zhao, B. Qiu, L.H. Guo, Z.Y. Lin, H.H. Yang, Ultraselective homogeneous electrochemical biosensor for DNA species related to oral cancer based on nicking endonuclease assisted target recycling amplification, Anal. Chem. 87 (2015) 9204–9208.
[24] S.F. Liu, C.F. Wang, C.X. Zhang, Y. Wang, B. Tang, Label-free and ultrasensitive electrochemical detection of nucleic acids based on autocatalytic and exonuclease III-assisted target recycling strategy, Anal. Chem. 85 (2013) 2282–2288.
[25] S.K. Silverman, Deoxyribozymes: selection design and serendipity in the development of DNA catalysts, Acc. Chem. Res. 42 (2009) 1521–1531.
[26] P. Miao, B.D. Wang, Z.Q. Yu, J. Zhao, Y.G. Tang, Ultrasensitive electrochemical detection of microRNA with star trigon structure and endonuclease mediated signal amplification, Biosens. Bioelectron. 63 (2015) 365–370.
[27] L.J. Bai, Y.Q. Chai, X.Y. Pu, R. Yuan, A signal-on electrochemical aptasensor for ultrasensitive detection of endotoxin using three-way DNA junction-aided enzymatic recycling and graphene nanohybrid for amplification, Nanoscale 6 (2014) 2902–2908.
[28] R.M. Kong, X.B. Zhang, L.L. Zhang, Y. Huang, D.Q. Lu, W.H. Tan, G.L. Shen, R.Q. Yu, Molecular beacon-based junction probes for efficient detection of nucleic acids via a true target-triggered enzymatic recycling amplification, Anal. Chem. 83 (2011) 14–17.
[29] F. Wang, C.H. Li, L.D. Sun, C.H. Xu, J.F. Wang, J.C. Yu, C.H. Yan, Porous single-crystalline palladium nanoparticles with high catalytic activities, Angew. Chem. Int. Ed. 51 (2012) 4872–4876.

Please cite this article in press as: Y. Wu, et al., Enzyme spheres as novel tracing tags coupled with target-induced DNAzyme assembly for ultrasensitive electrochemical microRNA assay, Analytica Chimica Acta (2016), http://dx.doi.org/10.1016/j.aca.2016.10.005

[30] L. Duan, X.H. Yan, A. Wang, Y. Jia, J.B. Li, Highly loaded hemoglobin spheres as promising artificial oxygen carriers, ACS Nano 6 (2012) 6897–6904.
[31] R. Levicky, T.M. Herne, M.J. Tarlov, S.K. Satija, Using self-assembly to control the structure of DNA monolayers on gold: a neutron reflectivity study, J. Am. Chem. Soc. 120 (1998) 9787–9792.
[32] N.Q. Jia, Q. Zhou, L. Liu, M.M. Yan, Z.Y. Jiang, Direct electrochemistry and electrocatalysis of horseradish peroxidase immobilized in sol–gel-derived tin oxide/gelatin composite films, J. Electroanal. Chem. 580 (2005) 213–221.
[33] L. Ferapontova, E. Gorton, Effect of pH on direct electron transfer in the system gold electrode–recombinant horseradish peroxidase, Bioelectrochemistry 55 (2002) 83–87.
[34] L. Zhang, Q. Zhang, X.B. Lu, J.H. Li, Direct electrochemistry and electrocatalysis based on film of horseradish peroxidase intercalated into layered titanate nano-sheets, Biosens. Bioelectron. 23 (2007) 102–106.
[35] T. Ferri, A. Poscia, R. Santucci, Direct electrochemistry of membrane-entrapped horseradish peroxidase. Part II: amperometric detection of hydrogen peroxide, Bioelectrochem. Bioenerg. 45 (1998) 221–226.
[36] W.Y. Zhu, X.P. Su, X.Y. Gao, Z. Dai, X.Y. Zou, A label-free and PCR-free electrochemical assay for multiplexed microRNA profiles by ligase chain reaction coupling with quantum dots barcodes, Biosens. Bioelectron. 53 (2014) 414–419.
[37] H.A. Rafiee-Pour, M. Behpour, M. Keshavarz, A novel label-free electrochemical microRNA biosensor using methylene blue as redox indicator: application to breast cancer biomarker microRNA-21, Biosens. Bioelectron. 77 (2016) 202–207.
[38] S. Bi, M. Chen, X.Q. Jia, Y. Dong, A hot-spot-active magnetic graphene oxide substrate for microRNA detection based on cascaded chemiluminescence resonance energy transfer, Nanoscale 7 (2015) 3745–3753.
[39] P. Zhang, Y. Zhuo, Y.Y. Chang, R. Yuan, Y.Q. Chai, Electrochemiluminescent graphene quantum dots as a sensing platform: a dual amplification for microRNA assay, Anal. Chem. 87 (2015) 10385–10391.
[40] W.J. Zhou, W.B. Liang, X. Li, Y.Q. Chai, R. Yuan, Y. Xiang, MicroRNA-triggered, cascaded and catalytic self-assembly of functional “DNAzyme ferris wheel” nanostructures for highly sensitive colorimetric detection of cancer cells, Nanoscale 7 (2015) 9055–9061.
[41] Q. Zhang, F. Chen, F. Xu, Y. Zhao, C.H. Fan, Target-triggered three-way junction structure and polymerase/nicking enzyme synergetic isothermal quadratic DNA machine for highly specific, one-step, and rapid microRNA detection at attomolar level, Anal. Chem. 86 (2014) 8098–8105.
[42] Q. Wang, Q. Li, X.H. Yang, K.M. Wang, S.S. Du, H. Zhang, Y.J. Nie, Graphene oxide–gold nanoparticles hybrids-based surface plasmon resonance for sensitive detection of microRNA, Biosens. Bioelectron. 77 (2016) 1001–1007.

Please cite this article in press as: Y. Wu, et al., Enzyme spheres as novel tracing tags coupled with target-induced DNAzyme assembly for ultrasensitive electrochemical microRNA assay, Analytica Chimica Acta (2016), http://dx.doi.org/10.1016/j.aca.2016.10.005